IEEE Access
Multidisciplinary | Rapid Review | Open Access Journal

Received 26 July 2023, accepted 25 August 2023, date of publication 1 September 2023, date of current version 19 September 2023.

Digital Object Identifier 10.1109/ACCESS.2023.3311369

RESEARCH ARTICLE

Improving Power Quality Problems of Isolated MG Based on ANN Under Different Operating Conditions Through PMS and ASSC Integration

AHMED HUSSAIN ELMETWALY[1], AZZA AHMED ELDESOUKY[2], HESHAM M. FEKRY[3], RAMY ADEL YOUNIS[1], ABDULWASA B. BARNAWI[4], Z. M. S. ELBARBARY[4], AND AHMED A. SALEM[5]

[1]The Higher Institute of Engineering at El Shorouk City, El Shorouk Academy, El Shorouk, Cairo 11837, Egypt
[2]Department of Electrical Power Engineering, Faculty of Engineering, Port Said University, Port Fuad 42526, Egypt
[3]Department of Electrical Engineering, Egyptian Propylene and Polypropylene Company, Port Said 42527, Egypt
[4]Electrical Engineering Department, College of Engineering, King Khalid University, Abha 61421, Saudi Arabia
[5]Department of Electrical Engineering, Faculty of Engineering, Suez Canal University, Ismailia 41522, Egypt

Corresponding author: Ahmed Hussain Elmetwaly (a.hussien@sha.edu.eg)

This work was supported by the Deanship of Scientific Research, King Khalid University, under Grant RGP2/309/44.

ABSTRACT Microgrid (MG) technologies assist the power grid in evolving to become more efficient, less polluting, and more resilient by addressing the requirements of energy users. However, several technological issues arise as a result of the unpredictability and difficulty in estimating the efficacy and regulation of the many renewable energy resources (RERs) incorporated in MGs. Two of the most significant of these issues are maintaining system stability and power quality, which necessitate to get better the performance of the MGs. The most difficult challenge, system stability, can be achieved with successful Power Management System (PMS). This paper proposes an effective PMS for an AC MG equipped with a diesel generator (DG), a permanent magnet wind generator (PMWG), and a solar photovoltaic (PV) panel Based on an adaptable Artificial Neural Network (ANN). The ANN weights are properly tuned via the Enhanced Bald Eagle Search (EBES) optimization algorithm to produce a stable system during the whole training period, achieve MG energy balance, reduce the usage of fossil fuel DG and maintain MG voltage stability. In addition, for keeping power quality, an adaptive series shunt compensator (ASSC) is described in this work, along with a developed integrative PID controller, where the latter's controller gains are ideally set utilizing the EBES optimization algorithm to perform adaptably with self-tuning when the operational circumstances of an MG change. various cases are displayed to test the strong of offered ASSC on harmonic mitigation, dynamic voltage stabilization, reactive power control and power factor correction. Moreover, comprehensive case study based on realistic on-site location for Zafarana region, Suez Gulf region of Egypt is proposed. Taking into account The changing nature of weather-related renewable energy, actual loads states and transient faults.

INDEX TERMS Photovoltaic (PV), power management systems (PMSs), permanent magnet wind generator (PMWG), artificial neural networks (ANNs), renewable energy resources (RERs).

I. INTRODUCTION

Based on the most recent International Energy Agency data in 2022, the number of people living in distant areas around the world without access to electricity will increase by about 20 million, reaching nearly 775 million [1]. In such areas, excessive usage of fossil fuels and diesel generators has resulted in greater pollution levels, and detectable climate changes, posing a severe danger to natural ecosystems. The topic of global CO_2 emissions from fuel combustion has gained extreme prominence; like worldwide emissions in 2022 were 33.8 billion tonnes [1]. These negative

The associate editor coordinating the review of this manuscript and approving it for publication was Ahmed F. Zobaa.

consequences have emphasized the necessity for the utilization of renewable energy resources (RERs), which not only provide major environmental advantages but also for power generation enhancement [2], [3]. Microgrids (MGs) are currently seen as an available solution for the integration of RERs at both distribution system and loads [4]. The usage of MGs enables RERs to work in isolation in the event of a main grid outage. This, in turn, aids in some significant advantages such as, the effective conversion from a passive network to an active network, regulated power flow management, dependable and reliable supply, and power quality improvement [5].

Proper control and coordination techniques among multiple RERs subsystems is the main challenge confronting MG performance [5]. Moreover, the control structure of MG operation, especially at the isolated mode, is distinguished from conventional central power plants by the well-designed power management strategy (PMS) [5], [6]. Many studies have been conducted on MG challenging issues such as reliability issues, power quality enhancement, optimal size, cost, energy management and coordination control between sources and loads [7], [8], [9], [10]. The adaptive neuro fuzzy inference system (ANFIS) with elephant herd optimization (EHO) method was used in [11] to accomplish the PM for an MG consisting of different RERs and a battery bank as Energy Storage System (ESS) under different load conditions. In Ref. [12], a reliable PMS for concurrent PV, FC, and wind turbine (WT) operation is presented. The authors in [13] describe an extensive management of an isolated microgrid with insufficient energy reserves during contingencies scenarios that might result in a full system outage, a DSM strategy was also used in [13] to increase the load sustainability considering the endurance of the ESS. Several studies have been conducted to date in order to create energy management tools for MGs employing metaheuristic techniques and multi-objective optimization procedures. Because of their search capabilities, such strategies are well established in facing difficult optimization issues like as the day-ahead MG's operation. a smart PMS for an MG based on ANFIS that includes a doubly fed induction generator DFIG powered by WT and PV in combination with DG is presented in [14].

Based on the artificial intelligent of EMS in hierarchical decentralized MG, The authors in [15] suggest an EMS scheme based on the marine predator algorithm (MPA) to handle power utilization efficiently with big hybrid distributed energy resources while improving PQ difficulties using an ADVR. In [16], an artificial intelligence-based energy management system was proposed for simultaneously lowering an MG's entire running cost and emissions. The genetic algorithm (GA) was used in ref [17] to solve an isolated MG size problem using a multi-objective optimization model that sought to reduce emissions and lifetime cost while optimizing renewable energy integration. the uncertainties elements caused by operation, electricity pricing, and power system outages that arise from the penetration of large renewable energy resources are considered a challenging issue in large scale MG, therefore the multi-MGs (MMGs) could be a promising solution in mitigation such these challenges [18], [19], [20], [21].

In spite the PMS benefits in islanded microgrids, limitations may affect their operation like; power quality issues such as voltage sag, swell, harmonics, three phase faults, and voltage imbalance happened because of RERs or load variation are regarded as significant challenges in power system operation; however, these issues are widely recognized in conventional centralized power systems, but they are becoming more prevalent with the high penetration of RERs, particularly in isolated MG.

There is a relation between the power quality issues and usage the power management systems in grid because of the needing of power management systems always to install a lot number of inverter and converters that consequently a lot of harmonics appears. The ASSC topology has attracted lots of attention due to its capacity to improve power quality problems. A discrete nonlinear stabilizer for UPQC in power networks with low inertia and islanded operational state was developed in [22] due to the numerous stability issues present compared to higher level grids. This method proved helpful in fixing reliability difficulties and enhancing MG PQ profiles. In [23], a hierarchical controller made up primary controller, and harmonics block was proposed to mitigate current and voltage harmonics. Furthermore, according to [24], combining UPQC with multi-microgrid systems can eliminate various forms of current and voltage harmonics.

Based on the research studies mentioned above, it seems that not enough effort has been made to establish a comprehensive management system for stand-alone MG based on Artificial Neural Network (ANN) during changes in weather conditions to achieve MG Power balance, reduce fossil fuel DG utilization, and maintain MG voltage stability. Furthermore, the suggested ASSC demonstrates its resilience in dealing with harmonic mitigation, dynamic voltage stability, reactive power compensation, and power factor enhancement due to the PQ challenges associated with MG operation. This work's key contributions may be summed up as follows:

1- Based on ANN, a smart robust PMS strategy for an isolated MG that integrates traditional and renewable resources is proposed.
2- EBES optimization is introduced as metaheuristic algorithm for a proper tuning the ANN weights in order to produce a stable system during the whole training period and therefore increasing the overall system performance.
3- The proposed system's performance with the ANN is investigated in a variety of realistic climatic scenarios that reflect daily fluctuations in solar irradiance, ambient temperature, and wind speeds.
4- The recently developed ASSC is investigated, revealing improved voltage sag, swell, three phase faults and harmonics. Moreover, THD conditions for the system are proven to improve the PQ problems.

TABLE 1. Monthly average meterological data for the Zafarana site for five years.

Month	Solar irradiation (W/m^2)	Wind speed at 50 m hub height $V_{(z)}$ (m/s)	Temperature T (°C)
Jan.	182.8	13.18	12.78
Feb.	220.7	13.18	14.98
Mar.	278.3	14.57	17.82
Apr.	312.5	14.58	21.10
May	337.4	14.92	25.52
June	361.2	15.66	27.97
July	353.5	14.54	29.24
Aug.	330.6	14.34	29.40
Sept.	294.2	14.51	27.21
Oct.	241.2	14.07	24.08
Nov.	196	12.44	19.73
Dec.	170	12.71	14.81
Annual average	273.2	14.05	22.05

5- As an evaluation of the performance of the employed system to mimic the specified ASSC's behaviors, a comparative analysis of moth flame (MFO), grey wolf optimization (GWO), and EBES techniques is offered.

The rest of the paper is structured as follows: the proposed system description is described in section II. Section III introduces the ASSC's operating principal where the control methodology of Active Power Filter (APF) and Dynamic Voltage Restorer (DVR) are investigated. The EBES procedures is studied in section IV. The simulation results and comments are presented in Section V. Finally, Section VI introduces the conclusions.

II. SYSTEM DESCRIPTION

The proposed MG is located in the Zafarana area of the Suez Gulf on Egypt's Eastern Red Sea coast, at 29′ 112″ and 32′ 6″ latitude and longitude angles, respectively. Monthly averaged sun irradiance, wind speed, and temperature data from NASA's Modern-Era Retrospective Analysis for Research and Applications (MERRA) [25] are gathered and summarized in Table 1 for a five-year period (2018-2022).

The connected load to the thoroughly tested MG is provided based on the Suez Canal Company for Electrical Distribution (CCED) as addressed in [26] with considerably reduced scaled values. The load profile represents normal variation of different local connected loads at Zafarana during a typical day.

Basically, the Zafarana site is divided mostly between residential and industrial zones. The load, as summarized in Table 2, consists of seven tourist villages, a hospital, a police station, and a bank, as well as some water pumping load for the tourist village landscape regions. The industrial area consists of three manufacturing industries, including heavy load industries and lighter manufacturing industries such as food processing and packaging, with an average daily load of 2.8 MW. Sun radiation and wind speeds are the key

TABLE 2. Tested mg's residential and industrial loads.

Type of Loads	Load Description		Average daily Load Values (kW)
Residential	Clinic Center	Services HVAC	250
	Compound1	Lighting & services	170
		HVAC	
	Compound 2	Lighting & services	180
		HVAC	
	Compound 3	Lighting & services	180
		HVAC	
	Compound 4	Lighting & services	200
		HVAC	
	Compound 5	Lighting & services	200
		HVAC	
	Compound 6	Lighting & services	200
		HVAC	
	Compound 7	Lighting & services	200
	Police Station	Services	250
	Bank	Services	
Industrial	Steel manufacturing	large Industrial	220
	Cement manufacturing (1)	large Industry	300
	Cement manufacturing (2)	large Industry	300
	Food manufacturing	Light manufacturing	150

contributors to the availability of solar and wind energy. The study is carried out in the Gabel El-Zeit, which is seen in Fig. 1 and is located in Egypt's North-Eastern Desert on the western coast of the Suez Gulf. Location coordinates were 33° 30' and 24° 55' E, and 27° 56' and 28° 10' N. Zafarana is considered one of the most suitable locations for applied the renewable energies technologies in Egypt for good wind speeds and solar radiation. The solar Atlas for Egypt mentioned in detail the average values of irradiance in chosen site from the mid and end of year that moves from 353.4 to 172.1 W/m^2 as displayed in Table 1. The proposed system's PMS is designed to target:

1. Stable MG voltage.
2. Power balance between the generation and demand.
3. Reduce DG fuel consumption to the lowest level.
4. Monitoring the maximum power point (MPP) of wind and solar resources.

These targets are accomplished through using a management system that anticipates the generated power from RERs and based on that computes the required mechanical power with the exact least quantity of diesel engine gasoline.

In general, the ANN is a learning-based clever system that integrates data processing skills. In a two-pass parameter updating procedure, the traditional hybrid learning algorithm

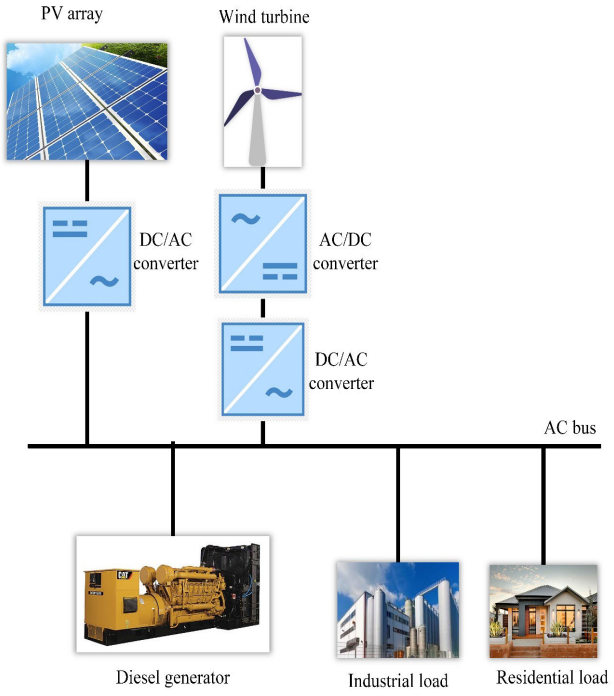

(a)

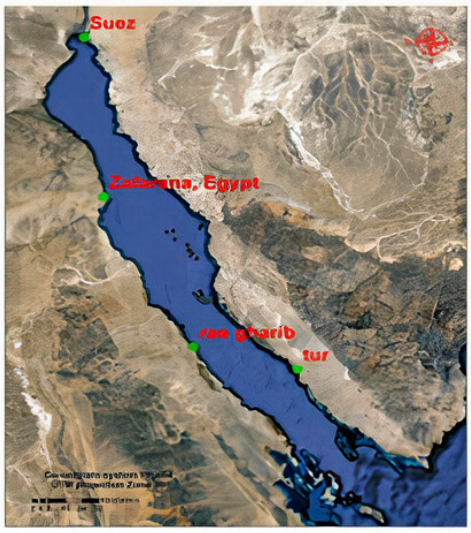

(b)

FIGURE 1. (a) The proposed system 's schematic diagram and (b) The system location on the map.

(HLA) for ANN combines gradient descent (GD) and least squares estimator (LSE). Three inputs and one output make up the suggested ANN's design. These are, wind speed, solar radiation and ambient temperature. The predicted mechanical power from the ANN is to be provided to the DG to complete the power needed to balance the electrical load. The suggested ANN, EBES-ANN controllers, are trained using 260 training examples. Ten arbitrary training examples are exposed in Table 3. The proposed system's schematic diagram and the real system location on map are depicted in Fig. 1.

TABLE 3. Ten random samples from ann training samples.

Input 1 Wind speed (m/s)	Input 2 Solar Irradiation (W/m^2)	Input 3 Ambient Temp. (°C)	Output Diesel Mech. Power (W)
8.5	1000	30	552800
7	800	25	825300
9.8	600	15	725600
12	650	30	435400
10.4	300	35	610200
4	800	40	875500
12	0	20	1054000
7.8	500	30	755000
9	0	15	1325900
8.6	1000	25	453650

III. THE PROPOSED ASSC

A. THE OPERATING PRINCIPAL OF ASSC

The proposed ASSC structure's exact construction is shown in Fig. 2. DVR refers to a full bridge converter that includes two half-bridge bi-directional voltage source converters, one with a shunt APF and one with a series APF. The shunt converter is connected to the series converter's left side. To get a clean sine spectrum for current (i_G) in phase with voltage (v_G), the shunt APF injects reactive and harmonic current (i_P) to compensate the distorted current (i_O). The current relationship is as follows:

$$i_G(t) = i_P(t) + i_o(t) \tag{1}$$

The grid voltage and current have the following relationships:

$$v_G(t) = \sqrt{2}V_G \sin \omega t \tag{2}$$

$$i_G(t) = \sqrt{2}I_G \sin \omega t \tag{3}$$

where ω represents the grid angular frequency. v_G & i_G represent grid voltage and current in steady-state expressed as root-mean-square (RMS) values, respectively. Between the v_G and the load voltage (v_O), the DVR can be viewed as a controlled voltage source (v_A). The voltages relationship is,

$$v_o(t) = v_G(t) + v_A(t) \tag{4}$$

The DVR converter, which regulates the voltage of the load, receives information about the controlled-out voltage from an incoming reference signal. To control the voltage delivered to the load, the reference signal's amount can be altered. The grid voltage should be fed in series with the series DVR to quickly compensate the difference between the nominal and real voltages. The required voltage should be always supplied to avoid variations, voltage sags, and flashing in case of dynamic voltage change.

For the load voltage, it can keep up a decent voltage quality with constant amplitude. In actuality, the DVR can be constructed using an inverter with a dc-ac voltage source as shown in Fig. 2. Energy is required to keep the compensating voltage at a steady level when the system is undervolted. As a result, to exchange power and balance the system's intake and output power, these two ac sources are linked using a dc link controller. By introducing current, serving as

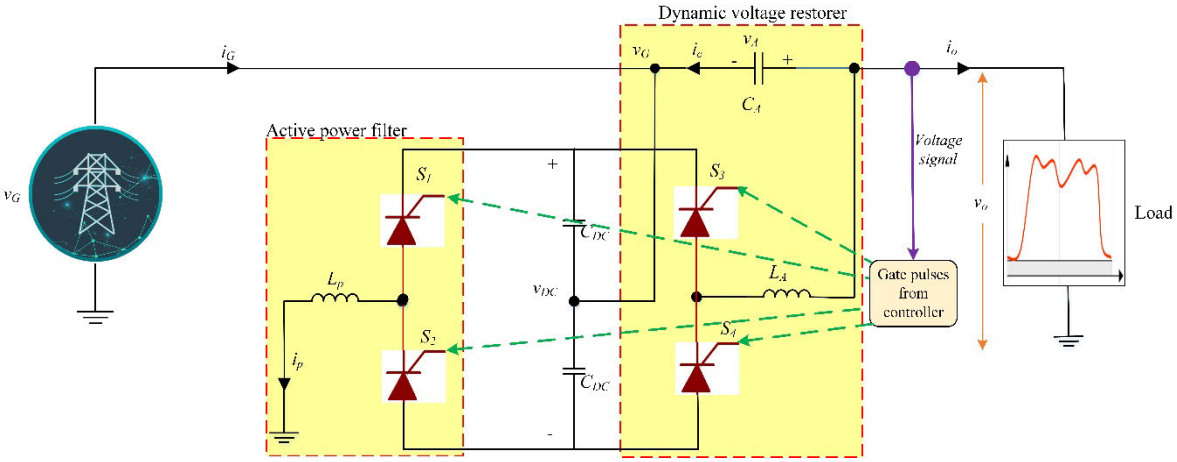

FIGURE 2. The proposed single-phase ASSC.

a rectifier, and filtering current, the APF VSC regulates the load's current harmonics. The DVR receives electricity via the DC connection as well.

For the load voltage, it can keep up a decent voltage quality with constant amplitude. In actuality, the DVR can be constructed using an inverter with a dc-ac voltage source as shown in Fig. 2. Energy is required to keep the compensating voltage at a steady level when the system is undervolted. As a result, to exchange power and balance the system's intake and output power, these two ac sources are linked using a dc link controller. By introducing current, serving as a rectifier, and filtering current, the APF-VSC regulates the load's current harmonics. The DVR receives electricity via the DC connection as well.

Thus, by changing the current amplitude linked to the grid, the dc link voltage manager regulates the dc link voltage (v_{DC}). Up until the dc link voltage hits steady-state, a fixed number, the system is safe. This implies an equal relationship between the incoming power (p_G) and outgoing power (p_O). In a steady condition, the powers are organized as follows:

$$p_G(t) = p_1(t) - p_2(t) + p_o(t) \tag{5}$$

Figure 2 depicts the three controllers that are connected to form the system in conclusion. The series DVR compensating method is meant to work under voltage sag circumstances. It must deliver a voltage that is in phase with the grid voltage. The supplied voltage will be out of step with the grid voltage to allow for a voltage swell.

B. ASSC'S CONTROL METHODOLOGY

In [27], it was suggested that the highly dominant PID controller could be replaced with active disturbance rejection controller (ADRC), which combines a partially model-based modern controller [28] with the PID controller and a state observer (SO) [29]. The purpose of using ADRC is to identify and counteract disturbances in the system by adjusting the necessary voltage to ensure that the load voltage remains within the allowable limits. This is achieved by utilizing an extended SO (ESO), and the output value of this SO is then fed into the controller, as shown in [28]. Figure 3 illustrates the ADRC system with the ESO. The ADRC scheme is applied to guarantee the state variables of the closed loop system to converge to the reference state with the help of the extended state observer by estimating the inertia uncertainty and external disturbance.

A feedback control system is employed to ensure that the output of the system follows a reference signal. The use of state feedback is contingent on the complete set of states being physically measurable within the system. However, if the internal state of the system, or its state variables, cannot be directly measured, an estimation of the states is required. This estimation is accomplished using a state observer or observer algorithm. A state observer can estimate the unknown state variables, and if it estimates all the system's state variables, it is called a full-order state observer; otherwise, it is referred to as a reduced-order state observer. The input to a state observer is the plant's input and output signals, and its output is an estimate of the plant's state vector. For observable systems, a system observer can be used to obtain the system's state vector, and the observer acts as a subsystem to reconstruct the plant's state vector.

Suppose the linear, time-invariant system's plant is defined by:

$$\left.\begin{aligned} \dot{x} &= Ax + Bu \\ y &= Cx + Du \end{aligned}\right\} \tag{6}$$

The mathematical model of the observer will be nearly identical, with the exception of an added term to account for the estimation error, which compensates for inaccuracies in matrices A and B. The estimation error, defined as the difference between the measured output and the estimated output, is taken into consideration. The observer's model can

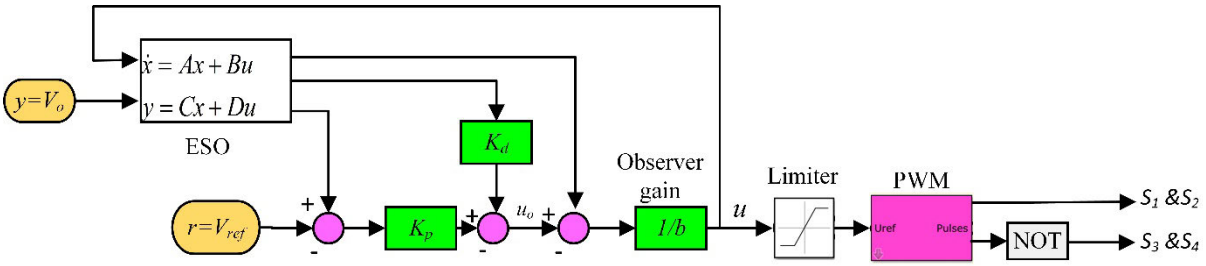

FIGURE 3. The proposed control ASSC.

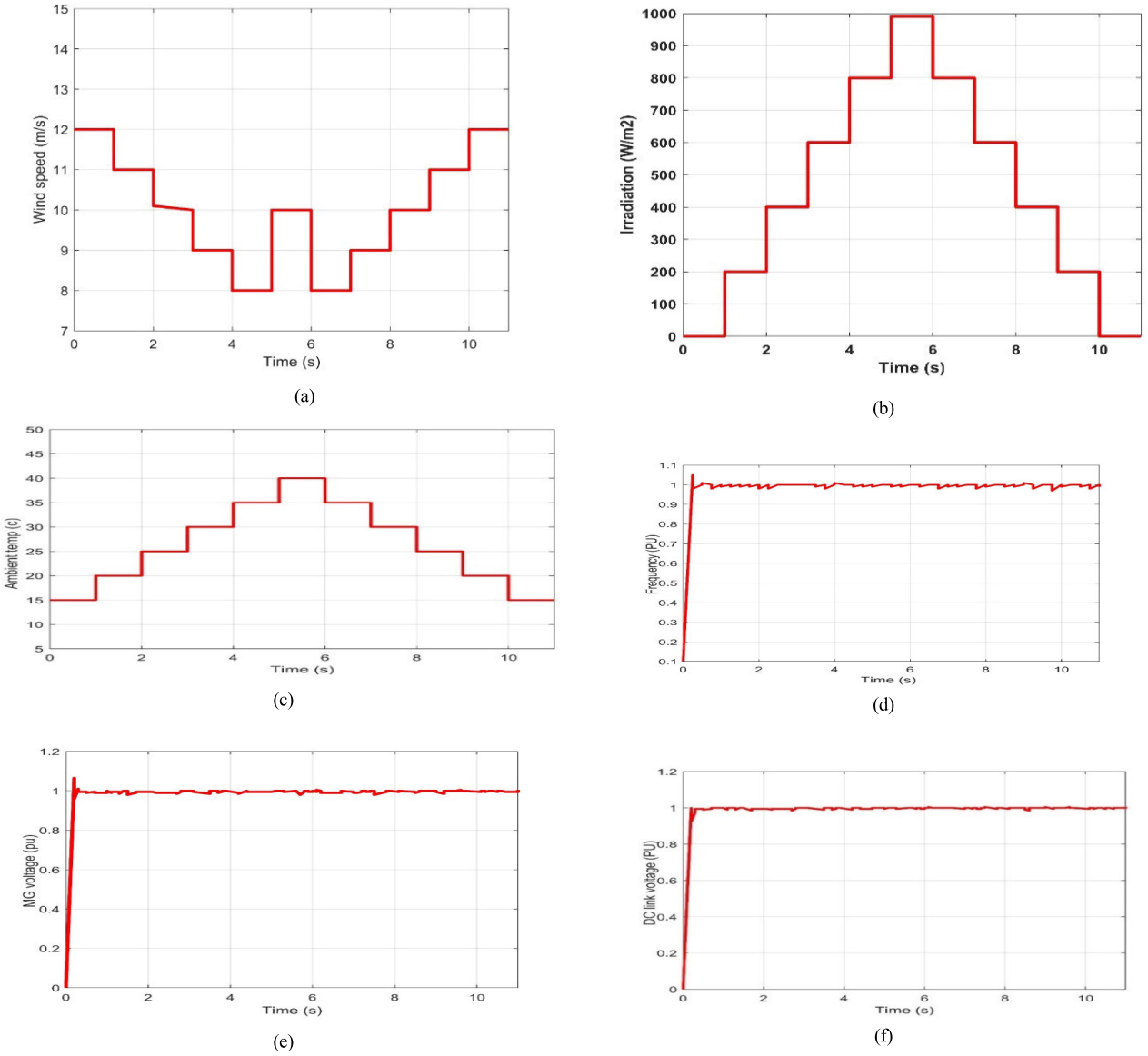

FIGURE 4. MG Response during variable weather conditions: (a) wind speed, (b) solar irradiation, (c) ambient temperature, (d) MG frequency PU, (e) MG voltage PU (f) DC link voltage PU.

be expressed as follows:

$$\dot{\hat{x}} = A\hat{x} + Bu + L\left(y - \hat{y}\right) \tag{7}$$

$$\dot{\hat{x}} = (A - L)\,\hat{x} + Bu + Ly \tag{8}$$

The estimated state of the system is denoted by $\hat{x}$, and the estimated output is represented by $C\hat{x}$. The observer takes the output y and control input u as inputs, and L is an observer gain matrix. In the case of an extended state observer

TABLE 4. The EBES optimization algorithm 's code.

Initialize the first population.
Assess the initial population's objective function.
While (the current iteration number < max. number of iterations)
Choosing the research space is the first stage.
For (each population i < population size)
$P_{new} = P_{best} + \alpha \times rand(P_{mean} - P_i)$
If $f(P_{new}) \prec f(P_i)$
$P_i = P_{new}$
If $f(P_{new}) \prec f(P_{best})$
$P_{best} = P_{new}$
End If
End If
End for
Stage 2: Looking around the chosen area
For (each population i < population size)
$P_{new} = P_i + y(i) \times (P_i - P_{i+1}) + x(i) \times (P_i - P_{mean})$
If $f(P_{new}) \prec f(P_i)$
$P_i = P_{new}$
If $f(P_{new}) \prec f(P_{best})$
$P_{best} = P_{new}$
End If
End If
End for
Stage 3: Swoop
For (each point i in the population)
$P_{new} = rand \times P_{best} + xl(i) \times (P_i - c1 \times P_{mean}) + yl(i) \times (P_i - c2 \times P_{best})$
If $f(P_{new}) \prec f(P_i)$
$P_i = P_{new}$
If $f(P_{new}) \prec f(P_{best})$
$P_{best} = P_{new}$
End If
End If
End for
Set k=k+1
End While

(ESO), both the internal dynamic uncertainties and external disturbances are considered as an additional state.

As a precise mathematical model of the system is unavailable, the following second-order system is used to represent the system.

$$\ddot{y} = bu + f(y, \dot{y}, w, t) \tag{9}$$

In the given system, y represents the output signal, u represents the input signal, w represents the external disturbance, b represents system parameters, and t represents time. The nonlinear system function $f(y, \dot{y}, w, t)$, or simply f, encompasses both disturbances and uncertainties and is commonly referred to as the total disturbance. In a distribution system, power quality can be affected by various disturbances such as voltage/current sags, voltage/current swells, and voltage/current imbalances. If these disturbances occur, they can lead to a reduction in the overall power quality. If the disturbance can be eliminated, the system would effectively become a double integral. Let $\hat{f}$ denote the estimate of the total disturbance

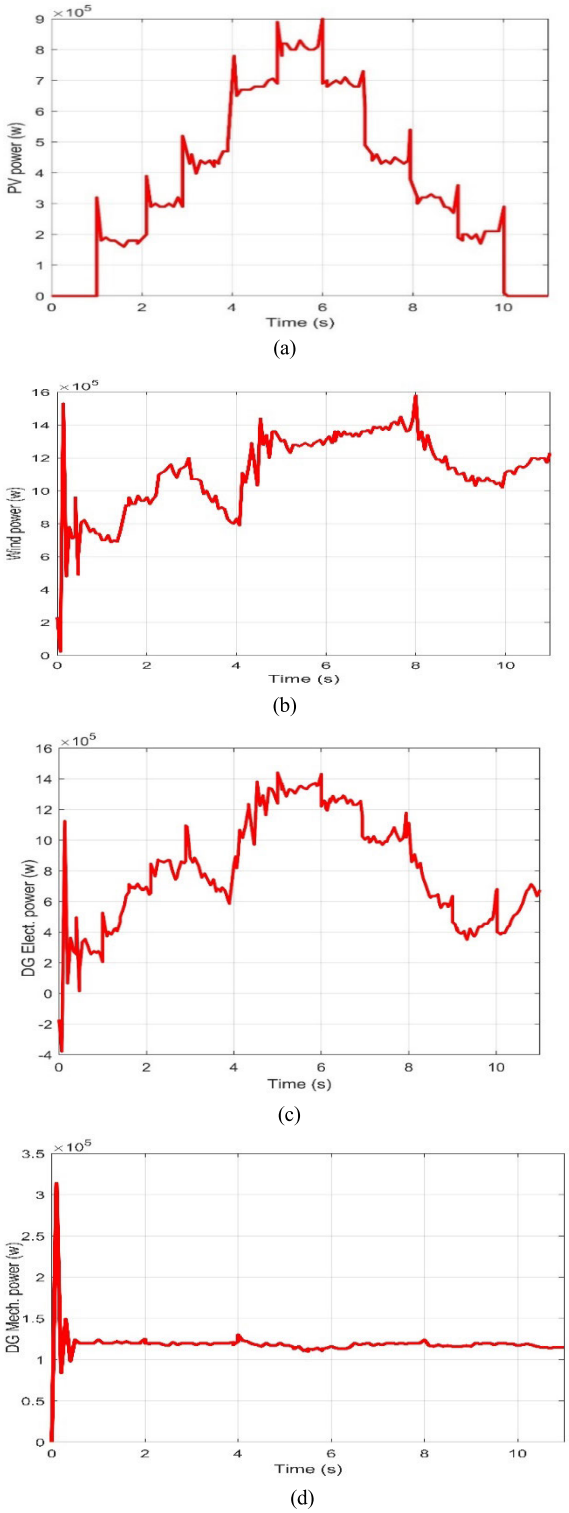

FIGURE 5. MG Response during variable weather conditions: (a) PV power, (b) WT power, (c) DG electrical power (d) mechanical DG power.

$f(y, \dot{y}, w, t)$ from Equation (9). The control signal is selected by:

$$u_o = bu + \hat{f} \tag{10}$$

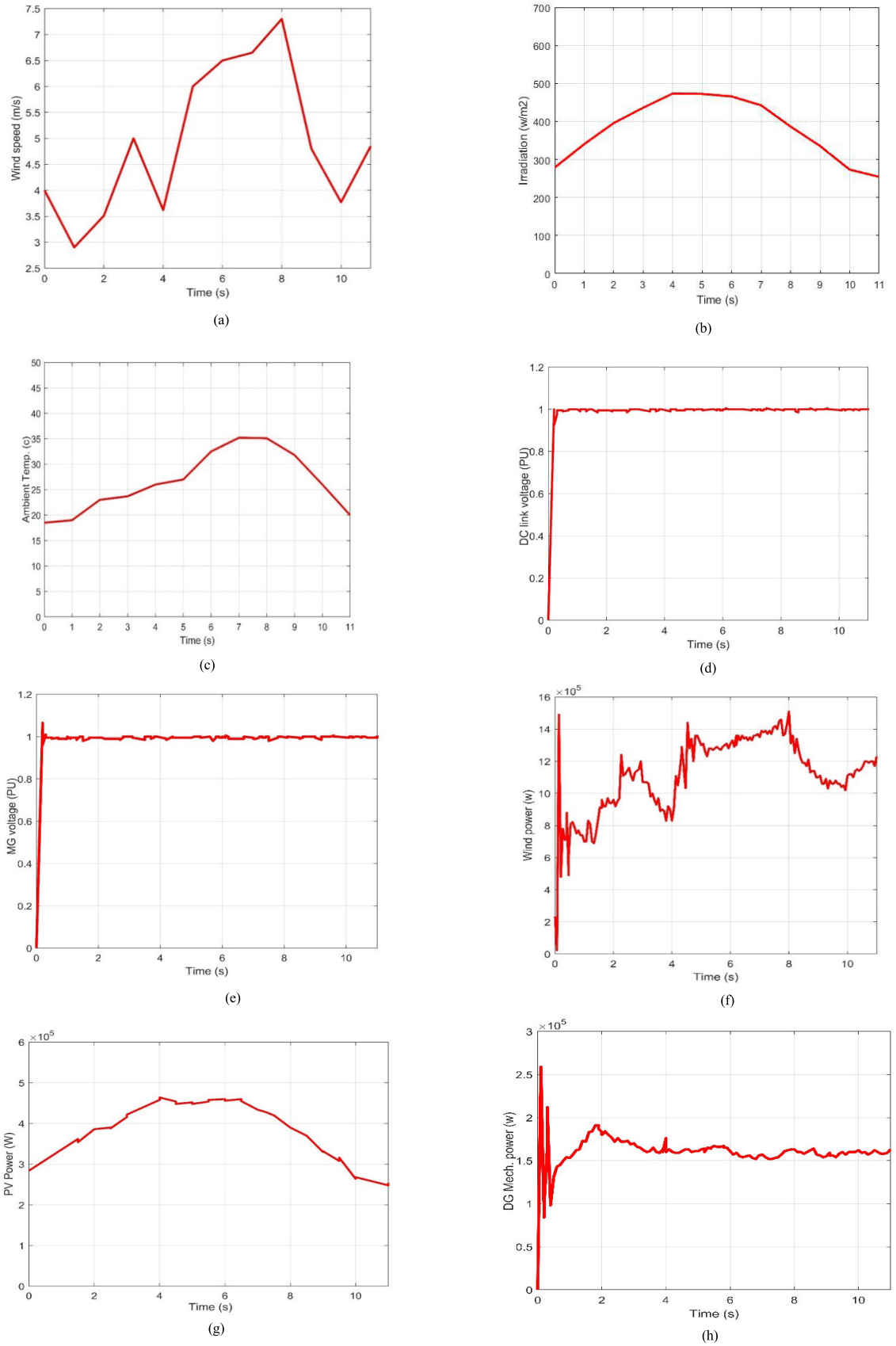

FIGURE 6. MG Response during variable weather conditions Case (ii): (a) wind speed, (b) solar irradiation, (c) ambient temperature, (d) DC link voltage PU, (e) MG Voltage PU, (F) WT power, and (g) PV power, (h) mechanical DG power (i) electrical DG power.

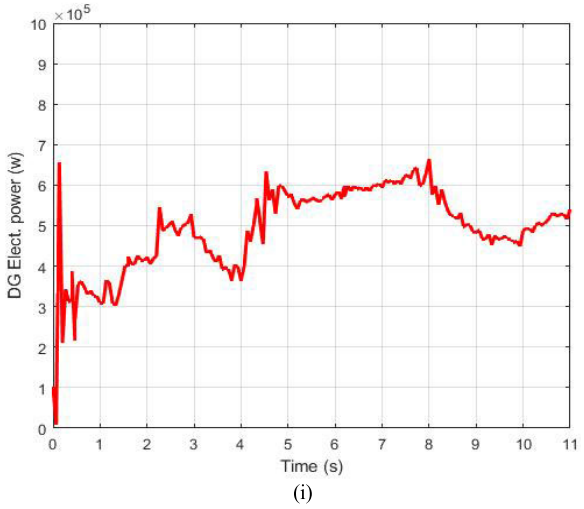

FIGURE 6. *(Continued.)* **MG Response during variable weather conditions Case (ii): (a) wind speed, (b) solar irradiation, (c) ambient temperature, (d) DC link voltage PU, (e) MG Voltage PU, (F) WT power, and (g) PV power, (h) mechanical DG power (i) electrical DG power.**

$$u = \frac{u_o - \hat{f}}{b} \tag{11}$$

Substituting u in Equation (9) gives:

$$\ddot{y} = u_o - \hat{f} + \hat{f} \tag{12}$$

So,

$$\ddot{y} \simeq u_o \tag{13}$$

Since the system would ideally become a pure double-integrator, a basic proportional derivative (PD) controller with input signal u_O should be adequate to regulate it.

$$u_o = K_p\,(r - y) + K_d\,(\dot{r} - \dot{y}) \tag{14}$$

where, K_p and K_d represent the proportional and derivative gains, respectively, of the PD controller and r denotes reference signal.

IV. EBES PROCEDURES

The EBES optimization algorithm is a kind of meta-heuristic algorithm which is based on natural principles. It uses the hunting strategies of the bald eagle as a bird model. The BES algorithm has three parts: selecting space, hunting in space, and swooping. The first part, selecting space, where the eagle chooses a place with the most prospective preys. The second part, hunting in space, where the eagle advances toward the chosen area's victims. The third part, swooping, involves the eagle taking off from the optimal location selected during the swooping phase and flying there. The EBES algorithm combines the advantages of both the evolutionary and swarm-based approaches [30]. Table 4 depicts the EBES optimization algorithm 's code. The new ASSC-PI controllers' gains are adjusted using the fitness function, which is stated as:

$$\min\,(J) = \min(ITAE) \tag{15}$$

$$ITAE = \int_0^\infty t\,|e_t|dt \tag{16}$$

where J : The suggested ASSC controller 's overall error

ITAE: An acronym for integral time absolute error. e_t : The error signal.

The following constraints apply to the optimization issue.

The THD of the current (THDi), calculated using (17), should be less than ($THD_{i,max}$) as per IEEE standard.

$$THD_i = \frac{\sqrt{\sum_{h=2}^{n} I_h^2}}{I_1} \tag{17}$$

$$THD_i \le THD_{i,\max} \tag{18}$$

V. SIMULATION RESULTS

A. CASE STUDIES FOR PMS

MATLAB/Simulink® platform is used to model and simulate the proposed methodology. the simulated system cleared in Fig. 1. contains WT controller, PV controller, and ANN controller are its three primary controllers. The primary MG bus voltage, 575 V, will always be maintained by the WT controller through regulation of terminal voltages. Additionally, it adjusts the DC-link voltage and maximizes the amount of energy generated by the available wind. The function of the PV controller is to extract the most power possible out of the available irradiation. The PV terminal voltage and current signals act as the inputs, and the boost converter gate receive pulses as the output. The ANN controller is also in responsible for reducing the DG's fuel usage to a minimum level. The ANN controller's inputs and outputs have already been described before. The performance of the suggested system with the ANN is first examined under several climatic settings that simulate the daily variations in solar irradiance, ambient temperature, and wind speed. To validate the mentioned system, two case studies are proposed as:

Case #1: Analysis of PMS using step data input.

Case #2: Analysis of PMS using realistic data input.

Case #1

The irradiance up to the max in the noon before declining till disappearing at night. Similar to this, the ambient temperature peaks in the middle of the day and troughs at night. From another point of view, the wind speed daily ranges are often modest and gradually increases as night falls. The simulation has also taken into account sudden change in wind speed, as illustrated in pattern from period t=5 to t=6 s. The step function is used in the changes of the three studied weather conditions on purpose in order to test the validity of the proposed system. As shown In Fig. 4(a), the profile wind movement simulation starts with 12 m/s then decrease to 8 m/s and finally returns to 12 m/s but it is going through a period of sudden upswing from 8 to 10 m/s. In Fig. 4(b), the profile irradiance simulation starts with 0 W/m2 then increase gradually to 1000 W/m2 and lastly returns to 0 W/m2. In Fig. 4(c), the temperature simulation starts with 15 c○ then increase gradually to 40 c○ and finally returns to 15 c○.

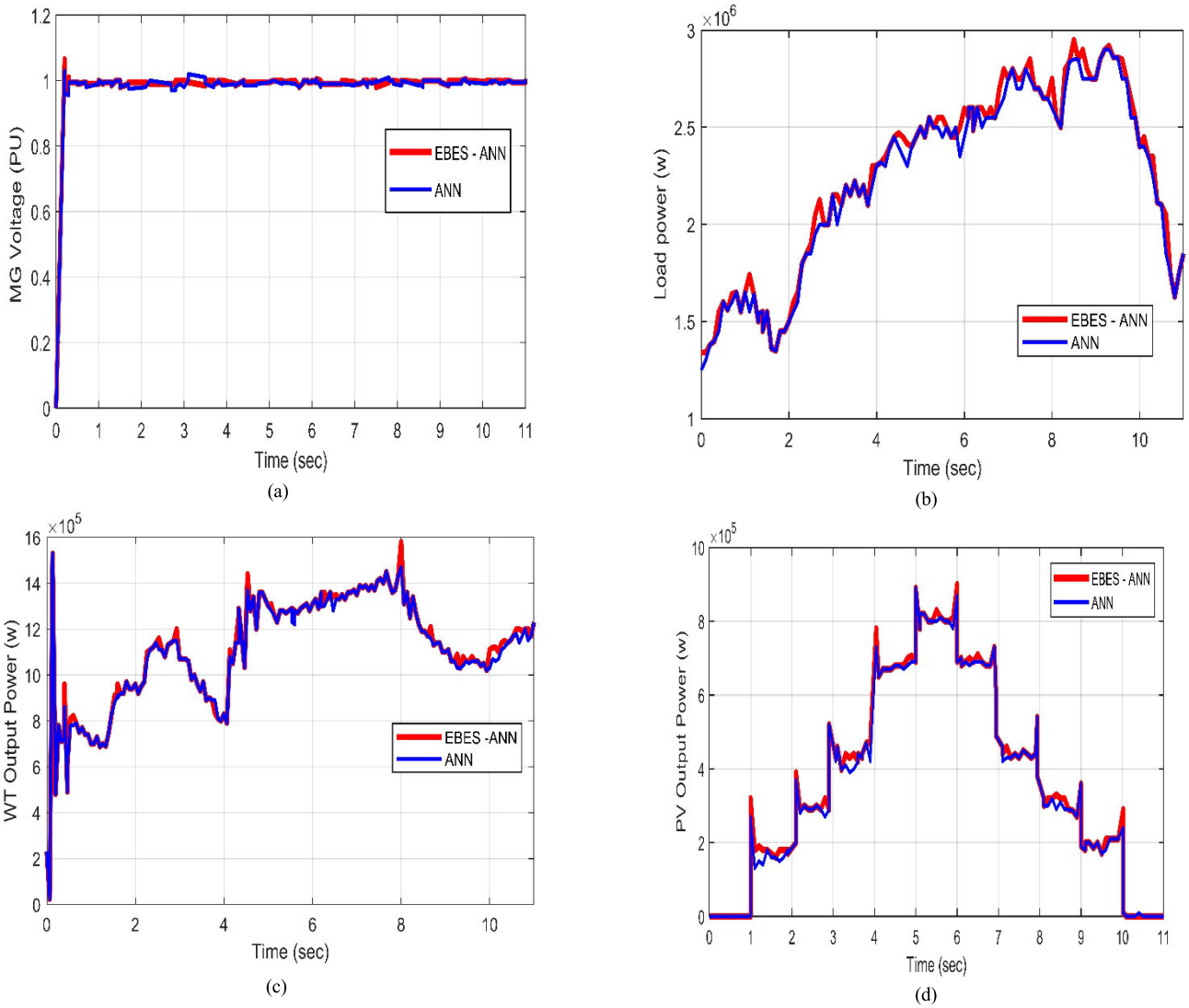

FIGURE 7. Comparison of the system performance during variable weather conditions using (EBES-ANN), and (ANN): (a) MG voltage PU, (b) Load Power, (c) WT output power MPP, (d) PV MPP.

The detailed power contribution in the MG from solar, wind, DG and the dispatched mechanical power from DG due to the ANN controller are shown in Fig. 5(a), 5(b), 5(c), and 5(d), respectively.

Case study #2:

To validate the proposed algorithm, actual real data are used for irradiation, wind speed, and ambient temperature as shown in Table 1.

Wind speed, irradiation, and ambient temperature of the selected case are shown in Figs.6 (a), (b), and (c) respectively. Figs. 6 (d), (e), show that changes in three parameters doesn't affect the values of either DC link or MG voltages. The error is always kept within acceptable range throughout the simulation period.

The power sharing scheme between the different power sources to supply the load is illustrated in Fig. 6. The WT, PV output and DG mechanical powers are displayed in Fig. 6(f), 6(g) and 6(h), respectively. However, Fig. 6(i) shows the electrical power generated by the DG as a result of ANN controller prediction.

TABLE 5. Comparison of the ADRC controller results under used techniques (case I).

Optimization techniques	MFO	GWO	Proposed (EBES)
Max. iteration	300	300	300
No. of population	50	50	50
Control parameters	$p = 0.75$	r1& r2 rand in [0,1]	c1& c2 rand in [1,2]
Computation time (s)	152.457	149.782	141.851
J_1 (Objective function)	1.714	1.797	1.582
K_p	1.8521	2.3574	1.8790
K_d	0.8965	1.7512	0.9524

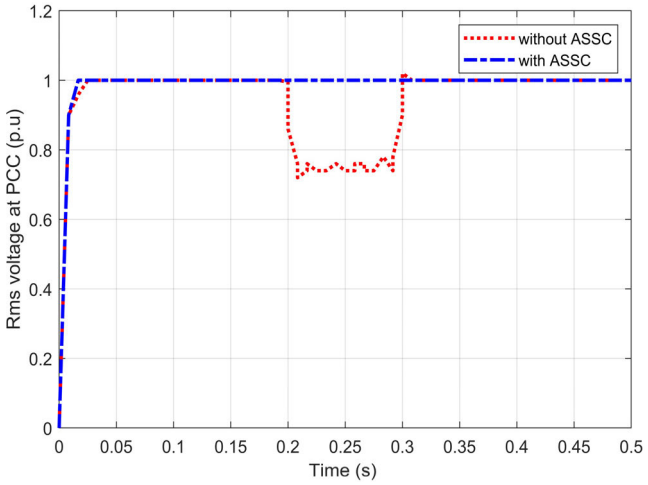

FIGURE 8. Case I Voltage sag results: Terminal voltage before and after compensation using ASSC.

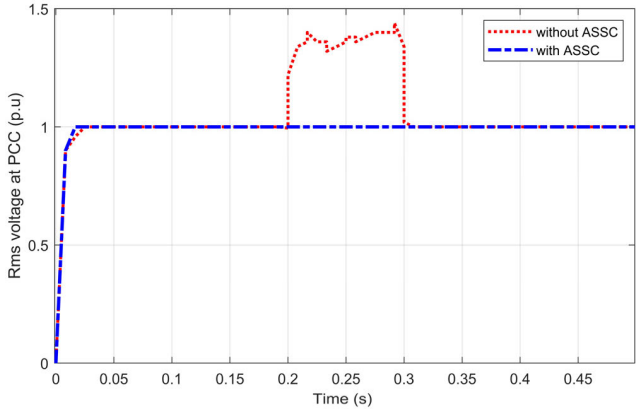

FIGURE 9. Case II Voltage swell results: Terminal voltage before and after compensation using ASSC.

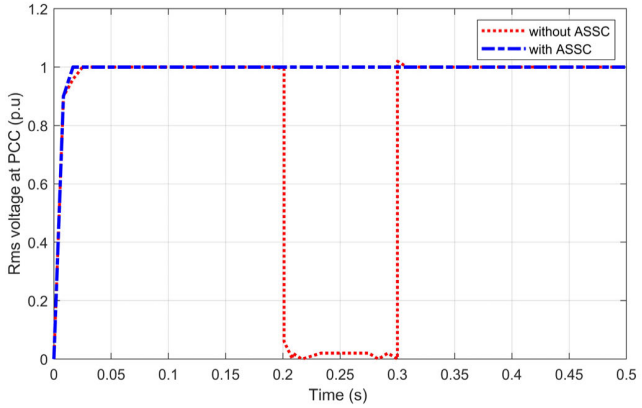

FIGURE 10. Case III Three phase fault results: Terminal voltage before and after compensation using ASSC.

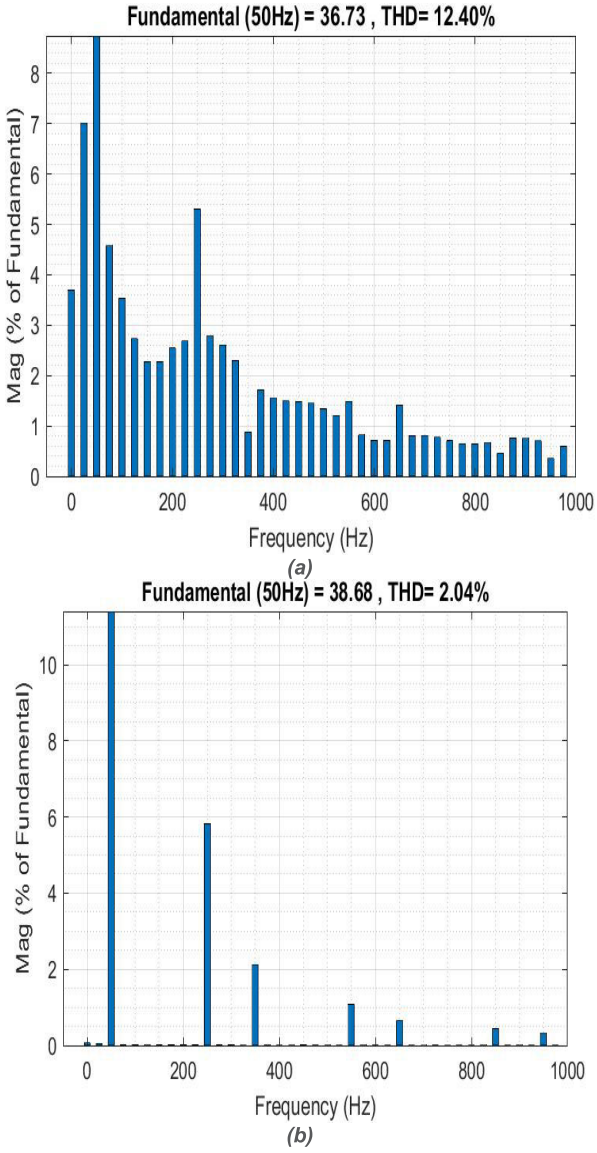

FIGURE 11. Case IV Analysis of harmonic distortion: THD for current before and after compensation.

An optimization algorithm (EBES) is implemented to drive the ANN. The results of (EBES-ANN) is compared to those of ANN. Fig. 7 displays the comparison of system performance in terms of load power, MG voltage, maximum power point (MPP) for both PV and WT. These are the four main criteria that can fully represent the efficiency of the system.

The MG voltage and load power stability with (EBES-ANN) are better than those of ANN as in Figs. 7(a) and (b). The MPP of WT and PV are nearly identical for these methods in Figs. 7(c) and (d). However, the (EBES-ANFIS) curve showed greater values than those of the ANN.

B. CASE STUDIES FOR PQ ENHANCEMENT USING ASSC

As illustrated in Fig. 2, the proposed ASSC is tested using the MATLAB/Simulink platform, regarding the enhancement of voltage sag, swell, and harmonics. In addition, THD conditions for the system are also studied. The parameters taken

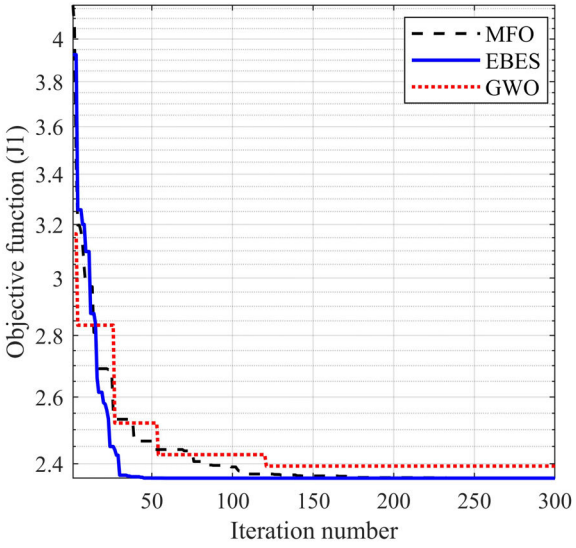

FIGURE 12. Convergence rates for Case I.

in the MATLAB/Simulink environment are mentioned in Table 5.

1) CASE I: VOLTAGE SAG

In this case, an overload occurs between 0.2 and 0.3 seconds, causing the grid voltage to drop to 50% of its maximum value. The ASSC was able to quickly recognize this sag state and injects the required output voltage to warranty a sinusoidal voltage to the load. The DC link has successfully restored the power that was injected into the parallel converter. Fig. 8 displays the voltage spectrum, before and after compensation, the load voltage distribution, and the necessary dispatched voltage.

2) CASE II: VOLTAGE SWELL

Sometimes, the tripping of bug loads leads to voltage swell. The swell mode was employed for this test from 0.2 to 0.3 seconds, and the voltage at the load terminals is increased to 140% of its RMS value. The ASSC was found to quickly recognize this swell state and absorbs the necessary output voltage magnitude to keep the stability and sinusoidal shape of the voltage load terminal. The DC link is coming out well restored the parallel converter's injected power. Fig. 9 displays the grid voltage spectrum, before and after compensation, the load voltage spectrum, and the required injected voltage.

3) CASE III: THREE PHASE FAULT

A three-phase fault occurs at the load bus in the time from t=0.2 s to t= 0.3 s. The DC link has successfully restored the parallel converter's injected power. Fig. 10 displays the grid voltage spectrum before and after compensation, the load voltage spectrum, and the required injected voltage.

4) CASE IV: ANALYSIS OF HARMONIC DISTORTION

THD is an important measurement for determining the degree of harmonic distortion affecting voltage or current waveforms. Fig. 11(a) shows THD_i computed for the output current, and Fig. 11(b) shows the measured THD_i of the input current after taking in consideration to assess the APF scheme's efficiency after implementation.

C. COMPARATIVE STUDY

A comparative analysis for the applied optimization methods action, moth flame (MFO), grey wolf optimization (GWO), and EBES methods are used by the ADRC controller to duplicate the attitudes of the offered ASSC typology. Table 5 displays the three algorithms with regard to Case I to mitigate the action of the proposed method. As per mentioned table, EBES constantly affects on the most suitable value of the objective function of 1.582 with 141.851 s which is considered rapid processing time. Figure 12 displays the convergence curve of EBES, MFO, and GWO techniques for Case I. These results illustrate that EBES influences the best values of the OF in the least number of iterations consistently.

VI. CONCLUSION

A smart PMS based on ANN has been proposed for a MG equipped with DG, PMWG, and PV panel. The EBES optimization algorithm has been utilized to fine tuning the ANN weights to accomplish different objectives with different climatic and fault conditions. The results clear that the offered strategy is durable and could successfully achieve its necessary objectives. The superiority of the (EBES-ANN) is validated compared with the (ANN). In addition, an ADRC controller with an EBES optimization algorithm has been designed for adaptive self-tuning performance when MG's operating conditions change along with ASSC to preserve power quality. Finally, under transient MG instabilities cases and faults conditions, the paper results show how the ASSC for PQ refinement succeed to keep the system robustness the power quality.

CONFLICT OF INTEREST

The authors declare that they have no conflict of interest concerning the publication of this article.

DATA AVAILABILITY STATEMENT

Data sharing is not applicable to this article as no datasets were generated or analyzed during the current study.

REFERENCES

[1] A. Pandey and M. Asif, "Assessment of energy and environmental sustainability in south Asia in the perspective of the sustainable development goals," *Renew. Sustain. Energy Rev.*, vol. 165, Sep. 2022, Art. no. 112492, doi: 10.1016/j.rser.2022.112492.

[2] Z. M. Ali, S. H. E. A. Aleem, A. I. Omar, and B. S. Mahmoud, "Economical-environmental-technical operation of power networks with high penetration of renewable energy systems using multi-objective coronavirus herd immunity algorithm," *Mathematics*, vol. 10, no. 7, p. 1201, Apr. 2022, doi: 10.3390/math10071201.

[3] M. Rawa, A. Abusorrah, H. Bassi, S. Mekhilef, Z. M. Ali, S. H. E. A. Aleem, H. M. Hasanien, and A. I. Omar, "Economical-technical-environmental operation of power networks with wind-solar-hydropower generation using analytic hierarchy process and improved grey wolf algorithm," *Ain Shams Eng. J.*, vol. 12, no. 3, pp. 2717–2734, Sep. 2021, doi: 10.1016/j.asej.2021.02.004.

[4] A. A. Abdelsalam, H. A. Zedan, and A. A. ElDesouky, "Energy management of microgrids using load shifting and multi-agent system," *J. Control, Autom. Electr. Syst.*, vol. 31, no. 4, pp. 1015–1036, Apr. 2020, doi: 10.1007/s40313-020-00593-w.

[5] X. Dou, X. Quan, Z. Wu, M. Hu, K. Yang, J. Yuan, and M. Wang, "Hybrid multi-agent control in microgrids: Framework, models and implementations based on IEC 61850," *Energies*, vol. 8, no. 1, pp. 31–58, Dec. 2014, doi: 10.3390/en8010031.

[6] Y. E. G. Vera, R. Dufo-López, and J. L. Bernal-Agustín, "Energy management in microgrids with renewable energy sources: A literature review," *Appl. Sci.*, vol. 9, no. 18, p. 3854, Sep. 2019, doi: 10.3390/app9183854.

[7] T. K. A. Brekken, A. Yokochi, A. von Jouanne, Z. Z. Yen, H. M. Hapke, and D. A. Halamay, "Optimal energy storage sizing and control for wind power applications," *IEEE Trans. Sustain. Energy*, vol. 2, no. 1, pp. 69–77, Jan. 2011, doi: 10.1109/TSTE.2010.2066294.

[8] R. A. Younis, D. K. Ibrahim, E. M. Aboul-Zahab, and A. El'gharably, "Techno-economic investigation using several metaheuristic algorithms for optimal sizing of stand-alone microgrid incorporating hybrid renewable energy sources and hybrid energy storage system," *Int. J. Energy Convers.*, vol. 8, no. 4, pp. 141–152, Jul. 2020, doi: 10.15866/irecon.v8i4.19137.

[9] A. H. Elmetwaly, A. A. ElDesouky, A. I. Omar, and M. A. Saad, "Operation control, energy management, and power quality enhancement for a cluster of isolated microgrids," *Ain Shams Eng. J.*, vol. 13, no. 5, Sep. 2022, Art. no. 101737, doi: 10.1016/j.asej.2022.101737.

[10] D. O. Koval, Y. Zhang, and A. A. Chowdhury, "Probabilistic wind energy modeling for electric generation system reliability assessment," in *Proc. IREP Symp. Bulk Power Syst. Dyn. Control VIII (IREP)*, Aug. 2010, pp. 1–9, doi: 10.1109/IREP.2010.5563301.

[11] R. Bhaduri, G. R. Saravana, and C. Vaskar, "Supervisory controller for power management of microgrid using hybrid technique," *Trans. Electr. Electron. Mater.*, vol. 21, no. 1, pp. 30–47, Feb. 2020, doi: 10.1007/s42341-019-00152-4.

[12] M. H. Mostafa, S. H. E. A. Aleem, S. G. Ali, A. Y. Abdelaziz, P. F. Ribeiro, and Z. M. Ali, "Robust energy management and economic analysis of microgrids considering different battery characteristics," *IEEE Access*, vol. 8, pp. 54751–54775, 2020, doi: 10.1109/ACCESS.2020.2981697.

[13] R. A. Younis, D. K. Ibrahim, E. M. Aboul-Zahab, and A. El'Gharably, "Power management regulation control integrated with demand side management for stand-alone hybrid microgrid considering battery degradation," *Int. J. Renew. Energy Res.*, vol. 9, no. 4, pp. 1912–1923, Dec. 2019, doi: 10.20508/ijrer.v9i4.10002.g7795.

[14] H. M. Fekry, A. A. Eldesouky, A. M. Kassem, and A. Y. Abdelaziz, "Power management strategy based on adaptive neuro fuzzy inference system for AC microgrid," *IEEE Access*, vol. 8, pp. 192087–192100, 2020, doi: 10.1109/ACCESS.2020.3032705.

[15] H. F. Sindi, S. Alghamdi, M. Rawa, A. I. Omar, and A. H. Elmetwaly, "Robust control of adaptive power quality compensator in multi-microgrids for power quality enhancement using puzzle optimization algorithm," *Ain Shams Eng. J.*, vol. 14, no. 8, Aug. 2023, Art. no. 102047, doi: 10.1016/j.asej.2022.102047.

[16] A. Chaouachi, R. M. Kamel, R. Andoulsi, and K. Nagasaka, "Multiobjective intelligent energy management for a microgrid," *IEEE Trans. Ind. Electron.*, vol. 60, no. 4, pp. 1688–1699, Apr. 2013, doi: 10.1109/TIE.2012.2188873.

[17] B. Zhao, Y. Shi, X. Dong, W. Luan, and J. Bornemann, "Short-term operation scheduling in renewable-powered microgrids: A duality-based approach," *IEEE Trans. Sustain. Energy*, vol. 5, no. 1, pp. 209–217, Jan. 2014, doi: 10.1109/TSTE.2013.2279837.

[18] B. Kroposki and G. Martin, "Hybrid renewable energy and microgrid research work at NREL," in *Proc. IEEE PES Gen. Meeting*, Jul. 2010, pp. 1–4, doi: 10.1109/PES.2010.5589753.

[19] S. Ali, S. A. A. Kazmi, M. M. Malik, A. H. U. Bhatti, M. Haseeb, S. M. R. Kazmi, and D. R. Shin, "Energy management in high RER multi-microgrid system via energy trading and storage optimization," *IEEE Access*, vol. 10, pp. 6541–6554, 2022, doi: 10.1109/ACCESS.2021.3132505.

[20] Y. Sun, Z. Cai, Z. Zhang, C. Guo, G. Ma, and Y. Han, "Coordinated energy scheduling of a distributed multi-microgrid system based on multi-agent decisions," *Energies*, vol. 13, no. 16, p. 4077, Aug. 2020, doi: 10.3390/en13164077.

[21] F. Fallahi, M. Yildirim, J. Lin, and C. Wang, "Predictive multi-microgrid generation maintenance: Formulation and impact on operations & resilience," *IEEE Trans. Power Syst.*, vol. 36, no. 6, pp. 4979–4991, Nov. 2021, doi: 10.1109/TPWRS.2021.3066462.

[22] T. O. Akinbulire, P. O. Oluseyi, and O. M. Babatunde, "Techno-economic and environmental evaluation of demand side management techniques for rural electrification in Ibadan, Nigeria," *Int. J. Energy Environ. Eng.*, vol. 5, no. 4, pp. 375–385, Dec. 2014, doi: 10.1007/s40095-014-0132-2.

[23] F. Boshell and O. P. Veloza, "Review of developed demand side management programs including different concepts and their results," in *Proc. IEEE/PES Transmiss. Distrib. Conf. Expo., Latin Amer.*, Aug. 2008, pp. 1–7, doi: 10.1109/TDC-LA.2008.4641792.

[24] A. H. Elmetwaly, R. A. Younis, A. A. Abdelsalam, A. I. Omar, M. M. Mahmoud, F. Alsaif, A. El-Shahat, and M. A. Saad, "Modeling, simulation, and experimental validation of a novel MPPT for hybrid renewable sources integrated with UPQC: An application of jellyfish search optimizer," *Sustainability*, vol. 15, no. 6, p. 5209, Mar. 2023, doi: 10.3390/su15065209.

[25] A. A. Salem, A. A. Eldesouky, A. A. Farahat, and A. A. Abdelsalam, "New analysis framework of Lyapunov-based stability for hybrid wind farm equipped with FRT: A case study of Egyptian grid code," *IEEE Access*, vol. 9, pp. 80320–80339, 2021, doi: 10.1109/ACCESS.2021.3085173.

[26] A. A. Salem, A. A. ElDesouky, and A. H. K. Alaboudy, "New analytical assessment for fast and complete pre-fault restoration of grid-connected FSWTs with fuzzy-logic pitch-angle controller," *Int. J. Electr. Power Energy Syst.*, vol. 136, Mar. 2022, Art. no. 107745, doi: 10.1016/j.ijepes.2021.107745.

[27] A. I. Omar, S. H. E. A. Aleem, E. E. A. El-Zahab, M. Algablawy, and Z. M. Ali, "An improved approach for robust control of dynamic voltage restorer and power quality enhancement using grasshopper optimization algorithm," *ISA Trans.*, vol. 95, pp. 110–129, Dec. 2019, doi: 10.1016/j.isatra.2019.05.001.

[28] D. Wei, C. Guo, Y. Shi, C. Guo, and J. Liu, "A new composite control strategy of space laser pointing mechanism based on active disturbance rejection controller," *IEEE Access*, vol. 11, pp. 21081–21091, 2023, doi: 10.1109/ACCESS.2023.3250941.

[29] J. Heidary, M. Gheisarnejad, and M. H. Khooban, "Stability enhancement and energy management of AC-DC microgrid based on active disturbance rejection control," *Electric Power Syst. Res.*, vol. 217, Apr. 2023, Art. no. 109105, doi: 10.1016/j.epsr.2022.109105.

[30] A. A. Abdelsalam, S. S. M. Ghoneim, and A. A. Salem, "An efficient compensation of modified DSTATCOM for improving microgrid operation," *Alexandria Eng. J.*, vol. 61, no. 7, pp. 5501–5516, Jul. 2022, doi: 10.1016/j.aej.2021.10.061.

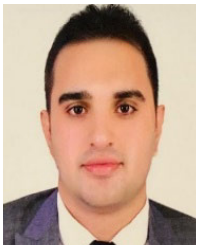

AHMED HUSSAIN ELMETWALY received the B.Sc. degree from The Higher Institute of Engineering, El Shorouk Academy, Cairo, Egypt, in 2008, and the M.Sc. degree from the Faculty of Engineering, Port Said University, Egypt, in 2015. He is currently an Assistant Professor with the Department of Electrical Engineering, The Higher Institute of Engineering, El Shorouk Academy. His current research interests include power quality, smart grids, power system analysis, and renewable energy.

AZZA AHMED ELDESOUKY received the B.Sc. and M.Sc. degrees in electrical engineering from Suez Canal University, in 1989 and 1995, respectively, and the Ph.D. degree from Bath University, U.K., in 2002. She is currently a Professor of electrical power engineering with Port Said University. She has authored more than 50 papers in journals and conferences. Her current research interests include power system operation and management, power quality, microgrid stability and control, smart grids, distributed generation systems, and AI applications in energy systems.

HESHAM M. FEKRY received the B.S. and M.S. degrees in electrical power and machines engineering from Cairo University, Giza, Egypt, in 2006 and 2012, respectively, and the Ph.D. degree in electrical engineering from Port Said University, Egypt, in 2021. He is currently the Electrical Section Head of Egyptian Propylene and Poly Propylene Company, which is considered one of the biggest petrochemical plants in the Middle East. His current research interests include power system operation and management, renewable energy, the generation and utilization of electrical power, microgrids stability and control, smart grids, energy management, and artificial intelligence applications in energy systems.

RAMY ADEL YOUNIS received the B.Sc. degree from The Higher Institute of Engineering, El-Shorouk Academy, Cairo, Egypt, in 2006, and the M.Sc. degree from the Faculty of Engineering, Helwan University, Egypt, in 2014. He is currently an Assistant professor with the Department of Electrical Engineering, The Higher Institute of Engineering, El Shorouk Academy. His current research interests include energy management, smart grids, power system analysis, and renewable energy.

ABDULWASA B. BARNAWI was born in Makkah, Saudi Arabia, in April 1981. He received the B.Sc. degree in electrical power engineering from the Yanbu Industrial College, Yanbu, Saudi Arabia, in 2007, the M.Sc. degree in electrical engineering from the University of New Haven, West Haven, CT, USA, in 2012, and the Ph.D. degree in electrical engineering from the Department of Electrical Engineering and Computer Science, The University of Toledo, Toledo, OH, USA, in 2016. Since 2019, he has been an Assistant Professor with the Department of Electrical Engineering, King Khalid University, Abha, Saudi Arabia. His current research interests include renewable energy integration, power system planning, generation adequacy evaluation, energy management (applying priced-based demand response strategies), smart grids, and dynamic electricity pricing.

Z. M. S. ELBARBARY was born in Kafrelsheikh, Egypt, in April 1971. He received the B.Sc., M.Sc., and Ph.D. degrees in electrical engineering from Menoufia University, Shebin El-Kom, Egypt, in 1994, 2002, and 2007, respectively. In 2009, he joined Kafrelsheikh University as an Assistant Professor. He was a Visiting Researcher with Ghent University, Ghent, Belgium, in 2016, for two months. He was promoted to a Full Professor of power electronics, in June 2022. His current research interests include the control of electrical machines, senseless control, the applications of power electronics, real-time control using digital signals processing, and renewable energy applications.

AHMED A. SALEM received the B.Sc. degree in electrical engineering from Suez Canal University, Ismailia, Egypt, in 2004, the M.Sc. degree in electrical engineering from Port Said University, Egypt, in 2012, and the Ph.D. degree in electrical engineering from Suez Canal University, in 2017. He is currently an Associate Professor with the Department of Electrical Engineering, Faculty of Engineering, Suez Canal University. His current research interests include flexible AC transmission systems (FACTS) technologies, microgrids, electric vehicles, and renewable energy-based distribution systems, with an emphasis on smart grid applications.